

## **Detection of fatigue crack growth in aircraft landing gear.**

Matthew G., Baxter, Dr Rhys, Pullin, Dr Karen M., Holford.  
School of Engineering, Cardiff University, UK

Keywords: Acoustic Emission, Fatigue Testing

### **Abstract**

Preliminary testing of a complete landing gear under fatigue test has demonstrated the applicability of the test using Acoustic Emission (AE) resonant sensors attached to the outer surface of the landing gear assembly. Attenuation trials were conducted which confirmed that attenuation through the main casing is low and provided data for optimisation of sensor positioning. Background noise levels were found to be well below the normal threshold used for detection of fatigue cracking.

Fatigue crack monitoring of compact test specimens has confirmed that AE can detect the initial stages of crack growth in typical landing gear materials. This study examines AE from fatigue cracks in compact tension (CT) specimens. 8 CT specimens were fatigue tested to failure and AE recorded throughout the test. The research has shown that detection of fatigue crack growth in CT specimens using appropriate AE techniques is possible. Two types of AE sensor were investigated and both confirmed to be appropriate for the detection of fatigue crack growth in the aerospace grade material. It would be preferable to use the higher resonant frequency sensor allowing more lower frequency emissions, relating to unwanted events, to be filtered out, however due to the smaller size of the miniature sensor and restrictions of access on the landing gear, both sensors will prove useful in the future of this project. Orientation of the sensors proved important, sensors orientated parallel to the crack growth recorded a significantly higher amplitude event than one perpendicular with the crack growth. It has proven possible to distinguish between emissions from a hydraulic actuator and fatigue crack growth in the laboratory.

### **Introduction**

For a landing gear system to be approved for use on commercial aircraft, each new design must undergo a lengthy fatigue test that simulates all in-service load cases. A typical fatigue test of a single landing gear consists of a life of 50000 flights, with 100 load cases per flight, with test duration of up to 5 years. A significant part of the test regime consists of scheduled breaks in testing to allow the landing gear to be removed, stripped and analysed for damage using conventional non-destructive testing techniques.

It is proposed that AE can be used to continuously monitor landing gear during fatigue testing and detect and locate damage as it occurs. Furthermore it is anticipated that the method can identify the type of damage, thus reducing the number and length of scheduled breaks and inspection. An additional benefit to AE monitoring is that the data can be correlated to load cycle information thus providing detail of the critical loads and cases that cause damage.

This paper forms part of the research undertaken by Messier-Dowty Ltd and Cardiff University to develop a 'health' monitoring system for the landing gear module whilst undergoing certification tests at Messier-Dowty Ltd. It aims to:

- Investigate 3 different sensors and assess their effectiveness in monitoring fatigue crack growth in aerospace grade steel.

- *Type I sensors* – A broadband displacement transducer that has a flat frequency response and allows undistorted AE signals to be recorded.
  - *Type II sensor* – A resonant sensor. By selecting the correct resonant frequency unwanted AE events such sources as hydraulic actuators can be filtered out without affecting the desired fatigue AE events.
  - *Type III sensor* – A miniature resonant sensor. Its smaller size allows it to be located in more confined spaces, however the resonant frequency is lower than that of the type II sensor.
- 
- Examine the effect of orientation of the sensor in relation to the crack growth. Type III sensors were used to compare results from perpendicular and parallel sensor orientation with respect crack growth. It was not possible to assess this effect on the type I and II sensors due to their larger size.
  - Compare AE from the hydraulic actuator with AE from fatigue crack growth. Type II sensors were used to record hydraulic actuator emissions and fatigue crack growth emissions.

## Experimental Procedure

**Specimen Details and Loading Procedure.** This investigation studied the AE released by fatigue crack growth in aerospace grade steel. Compact tension (CT) test specimens were designed in accordance with guidelines laid out by British Standards (BS 1998) (Figure 1).

The specimens were installed into the test rig as shown in Figure 2. The specimens were loaded using a 250 kN dynamic actuator governed by a Dartek 9500 control unit. Loads were applied using a sinusoidal waveform. Specimens were subjected to a load cycle calculated in accordance with British Standards (BS 1998).

**Instrumentation.** The AE sensor arrangement is shown in Figure 3. The sensors were mounted via an acoustic couplant layer of silicone grease and held in position with electrical tape. Sensor sensitivity was evaluated using the pencil lead fracture (PLF) technique (Hsu 1979, ASTM 1994).

Surface wavespeed, attenuation and location were assessed by conducting PLF's either side of sensors 2 and 3 on a CT specimen. The emissions were recorded at both sensors to evaluate the response. PLF's were conducted at three points between sensors 2 and 3 to evaluate the location accuracy.

AE activity was recorded using Physical Acoustics software on a 16 channel DiSP system. A 60dB threshold was used on all specimens. Optical crack length measurements were taken at various intervals during testing with a travelling microscope for 3 specimens. For all other specimens, metal foil gauges (KRAK GAGE) (RUMUL 2003) were used to automatically record crack growth. Both load and crack length were recorded as time-driven and hit-driven parametrics. All specimens were tested to failure.

## Results and Discussion

Response of the type I sensors to PLF's was above 90 dB and that the response from the type II and III sensors was above 97dB. This demonstrates that all sensors were mounted correctly. The arrival times and amplitude response from the wavespeed and attenuation

assessment allowed the wavespeed and attenuation to be calculated. The average wavespeed for 10mm thick plate was calculated at 4500 m/s. The attenuation was negligible. Figure 4 shows accurately located PLF's between sensors 2 and 3 sensors to within 10mm of the source.

To ensure that the data analysed during this research originated from the fatigue crack growth, only events occurring in the top 10% of load were considered. This not to say that fatigue would not occur below this level, only that it is likely to be the only active AE mechanism in the top 10% of load (i.e. there will be no crack closure or crack face rubbing). Figure 5 shows an example plot of cumulative wave parameters (counts, hits and absolute energy) against load cycles, compared with crack growth. In general, all wave parameters closely follow the trends of the crack growth throughout the load cycle, suggesting that the emissions collected are linked directly to the crack growth. However, the experiments that had their load cycle disrupted for optical crack measurements to be taken, displayed deviations from this trend with surges in AE at points with little or no crack growth. It is assumed that removal and re-installation from and to the test rig caused these anomalies.

**Type I Vs. Type II sensors.** AE from fatigue crack growth was recorded during each test. Feature data (absolute energy, duration, rise time, initiation frequency and counts) plotted against amplitude (an example is shown in figure 6). Recorded emissions by type I and type II sensors are compared. The type I sensor recorded fewer hits than the type II sensor, this is due to the lower sensitivity of the type I sensor. There is no significant difference in the pattern of feature data recorded by either sensor. This suggests that the type II sensor is suitable to use for recording AE from fatigue in these CT specimens. The resonant frequency has not had a major affect on the recorded AE in the CT specimen.

**Type I Vs. Type III sensors.** AE from fatigue crack growth was recorded during each test. Feature data (absolute energy, duration, rise time, initiation frequency and counts) plotted against amplitude (an example is shown in figure 7). Recorded emissions by type I and type III sensors are compared. The type I sensor recorded fewer hits than the type III sensor, this is due to the lower sensitivity of the type I sensor. There is no significant difference in the pattern of feature data recorded by either sensor. This suggests that the miniature resonant sensor is suitable to use for recording AE from fatigue in these CT specimens. The resonant frequency has not had a major affect on the recorded AE in the CT specimen.

**Parallel Vs Perpendicular located sensors.** AE from fatigue crack growth was recorded during each test. Feature data (absolute energy, duration, rise time, initiation frequency and counts) plotted against amplitude (an example is shown in figure 8). Emissions from type III sensors parallel and perpendicular with the crack growth are compared. There is no significant difference between the feature data recorded by either sensor. This showed that the parallel and perpendicular type III sensors produced similar feature data when recording AE from fatigue from a CT specimen. This suggests that the orientation of the type III had little affect on the feature data recorded during the test. However, on closer inspection the parallel sensor recorded events at 12 dB higher than the perpendicular sensor. A review of all specimens revealed this to be a common occurrence. This suggests that it is preferable to locate sensors parallel to the suspected fatigue fracture.

**Actuator Emissions Vs. Fatigue Emissions.** AE from fatigue crack growth was recorded during each test. Feature data (absolute energy, duration, rise time, initiation frequency and counts) was plotted against amplitude (an example is shown in figure 9). Emissions from two

type II sensors, one mounted on the actuator and one mounted on the specimen, are compared. Emissions recorded from the actuator have different feature data to those recorded from the specimen. Region 1 shown in figure 9 isolates all emissions from the actuator based on absolute energy. Region 2 in figure 9 isolates all emissions from the actuator due to a exceptionally long duration, a characteristic of acoustic noise. Region 3 in figure 9 isolates all actuator emissions based on a high number of counts. These three features allow easy identification of any actuator noise present in other tests. The waveform from the actuator is significantly different to the classical fatigue waveform (figure 10), the actuator waveform (figure 11) is continuous and displays no obvious peak. These results show that it easy to discriminate between actuator and fatigue emissions during these tests.

**Linear Location.** Using a wavespeed of 4500 m/s, figure 12 shows events located between two type III sensors. Most events are located at the centre of the array, where the crack is present, confirming the AE is from the crack. Due to the size of the specimen, there are inherent problems with location due to reflections and the size of the sensors, compared to their spacing. Signals that locate within 10 mm of the centre are regarded as well located. Events located either side of the 20 mm central band have been attributed to interaction between the specimen and the loading pins.

Figure 13 shows results from two periods of loading during test. The absolute energy recorded from the first 0 – 2000 cycles is much higher than the negligible amount received from 4000 – 6000 cycles. This directly corresponds to the amount of crack growth recorded, 0.67 mm and 0 mm respectively. This further confirms that the AE being recorded is from fatigue crack growth, and not from other sources.

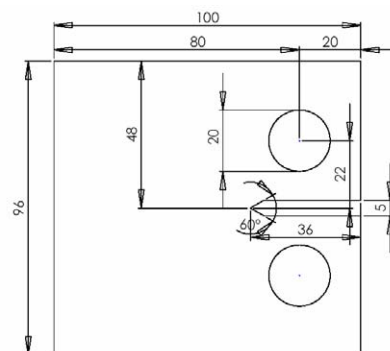


Figure 1 : Illustration of CT specimen geometry (dimensions in mm)

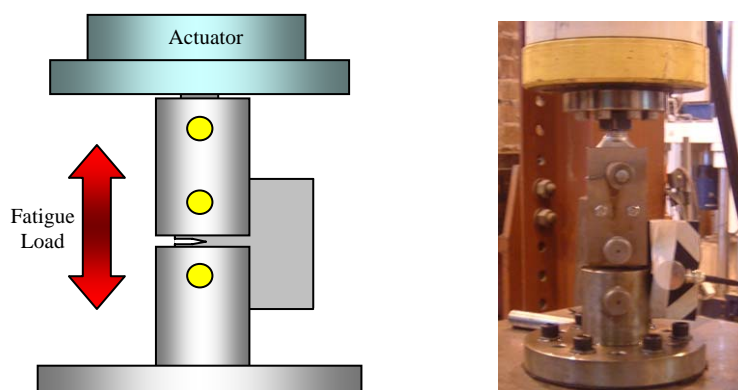


Figure 2 : Illustration and photograph of CT Specimen in the Test Rig

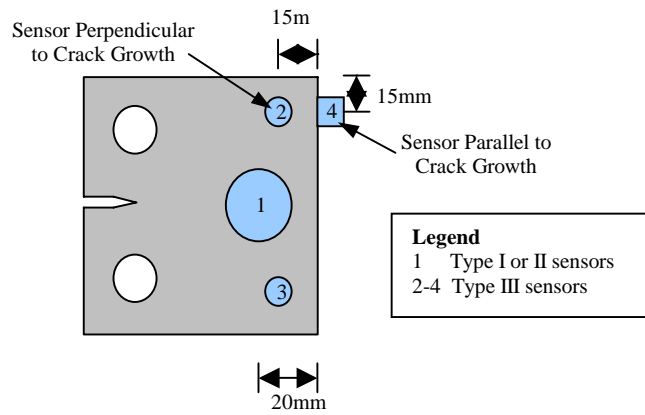


Figure 3 : Sensor Arrangement

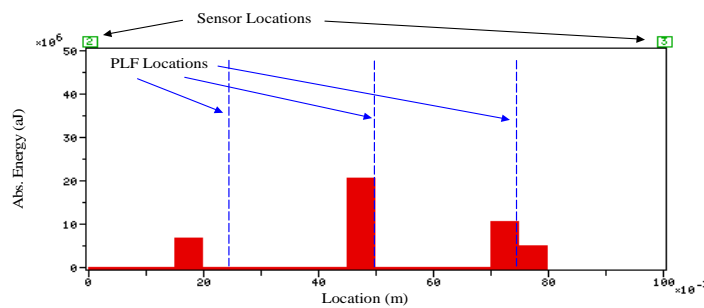


Figure 4 : Location of PLF's between Two Sensors

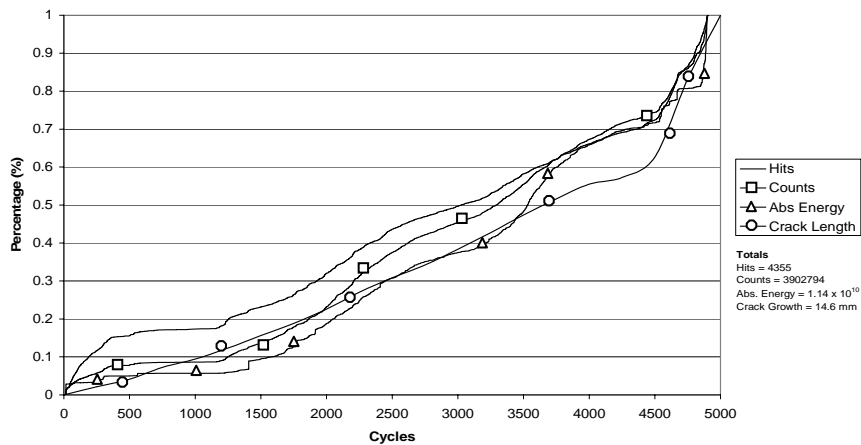


Figure 5 : Cumulative Feature Data against Crack Growth (Sensors 2 and 3)

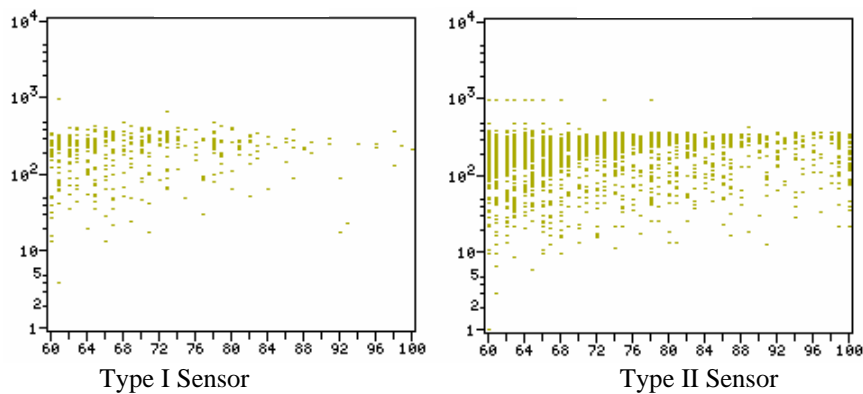
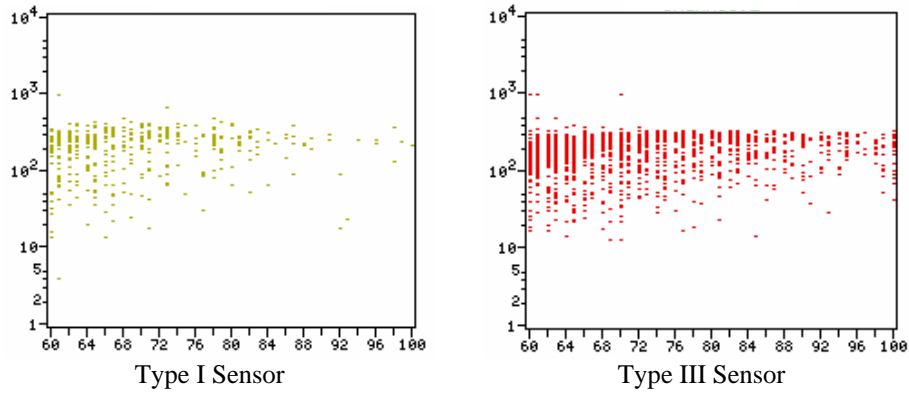
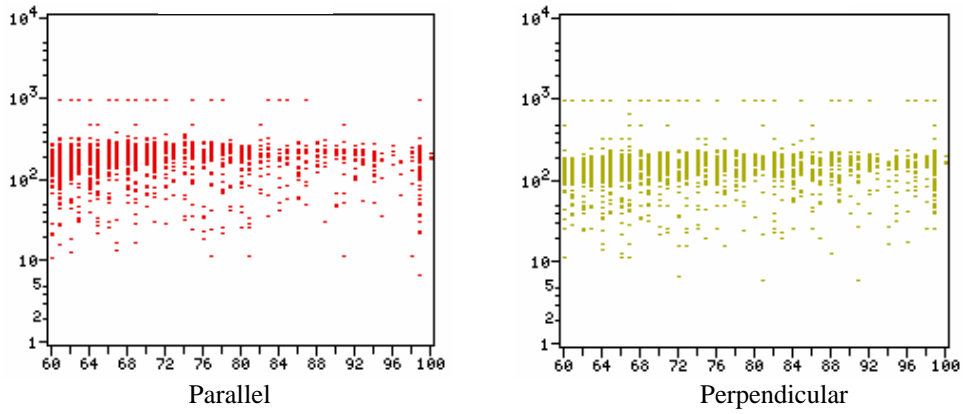


Figure 6 : Feature Data, Initiation Frequency against Amplitude



**Figure 7 : Feature Data, Initiation Frequency against Amplitude**



**Figure 8 : Example of Feature Data, Initiation Frequency against Amplitude**

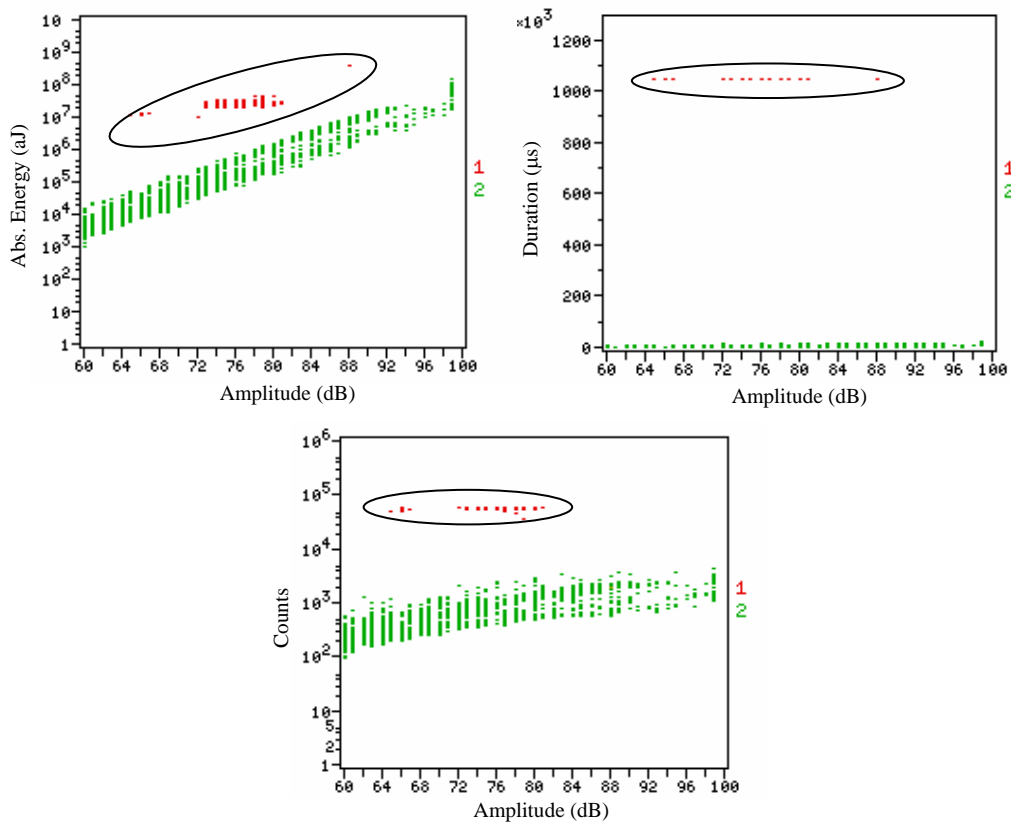


**Figure 9 : Feature Data from MDCT05**

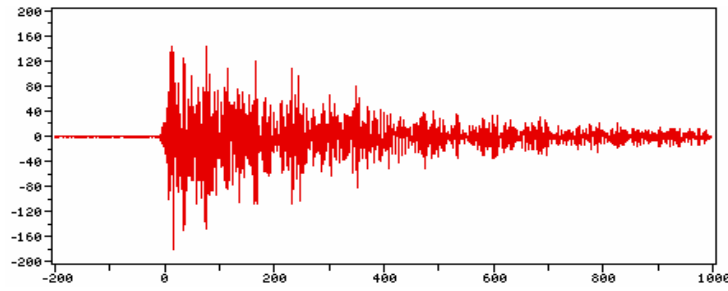


Figure 10: Waveform from Fatigue (Type II)

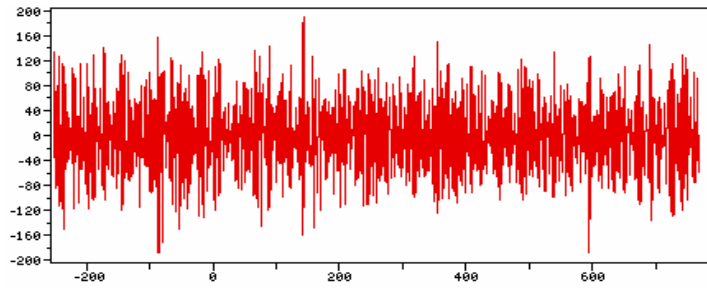


Figure 11 : Waveform from Actuator (Type II)

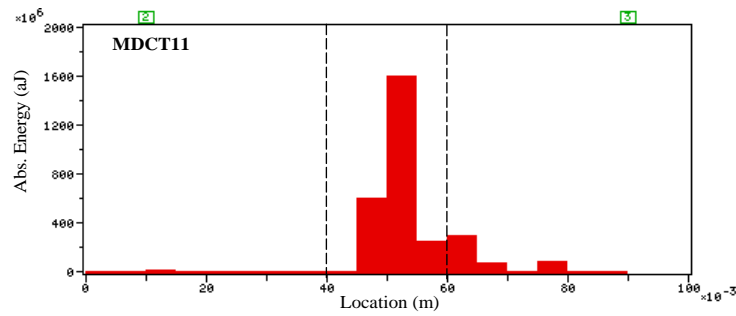


Figure 12 : Example Linear Location on a CT specimen

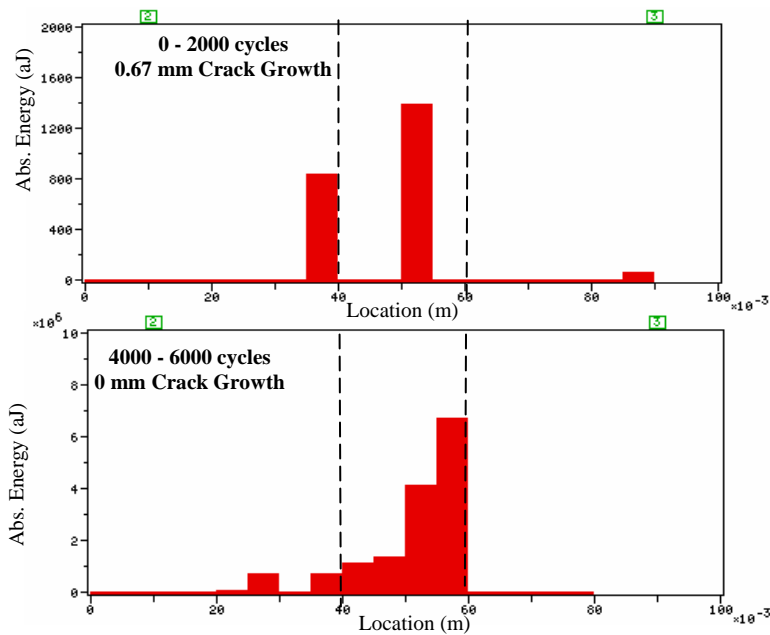


Figure 13: Linear Location of Crack Growth

### **Conclusions and Further Work**

This investigation has provided the basis for a `database` of AE waveforms from fatigue crack growth. The research has shown detection of fatigue crack growth in aerospace grade steel CT specimens using appropriate AE techniques to be possible. Two types of sensor, were investigated and confirmed to be appropriate for the detection of fatigue crack growth in aerospace steel. Orientation of the sensors proved important, a type III sensor orientated in parallel with the crack growth recorded a significantly higher amplitude event than one perpendicular to crack growth. Furthermore a quick and efficient way to distinguish between emissions from a hydraulic actuator and fatigue crack growth in the laboratory has been identified.

The work covered by this research has provided encouraging results, however further investigation is needed to further the main aim of producing a 'health' monitoring system for Messier-Dowty landing gear qualification tests.

The size of the CT specimens presented many problems from mounting of the sensors to wave reflections within the small plate. Location on such a small plate proved difficult and unrealistic. The theoretical error for time of arrival linear location is based on one wavelength of the emission, this results in an error of 36 mm. However greater accuracy was observed during this research. Larger specimens would allow greater understanding of wave attenuation and provide more realistic conditions.

The specimens were pre-cracked due to the heat treatment procedure, this allowed emissions to be collected from fatigue crack propagation (stage 2 fatigue). Research investigating the possibility of detecting fatigue crack initiation (stage 1 fatigue) needs to be conducted. Previous investigations reported that Messier-Dowty experience fatigue failure from particular geometric features, investigating fatigue crack growth initiating from similar features would provide more realistic results.

### **Acknowledgements**

Messier-Dowty Ltd who financially support this research.  
Physical Acoustics Ltd for their advice and technical support.

### **References**

ASTM (1994) Standard guide for determining the reproducibility of acoustic emission sensor response, American Society for Testing and Materials, E 976

BS (1998) Methods for Determination of the Rate of Fatigue Crack Growth in Metallic Materials, British Standards, BS 6835-1:1998

Hsu, N. N., and Breckenbridge, F. R. (1979). "Characterization and Calibration of Acoustic Emission Sensors." Materials Evaluation **39**: 60-68.

RUMUL (2003) <http://www.rumul.ch>, February 2004